Effect of perivascular electromagnetic flow probes on pulmonary hemodynamics

BRYDON J. B. GRANT, LINDA J. PARADOWSKI, AND JAMES M. FITZPATRICK
Department of Medicine, State University of New York at Buffalo, Buffalo, New York 14215

GRANT, BRYDON J. B., LINDA J. PARADOWSKI, AND JAMES M. FITZPATRICK. *Effect of perivascular electromagnetic flow probes on pulmonary hemodynamics.* J. Appl. Physiol. 65(4): 1885–1890, 1988.—We determined the effect of perivascular electromagnetic flow probes (EMF) on pulmonary hemodynamics in acute experiments. In seven dogs placement of the EMF on the main pulmonary artery (MPA) increased pulmonary arterial pulse pressure by 25% (17.8–21.9 cmH_2O, $P < 0.005$) and mean right ventricular pressure by 12% (23.2–25.9 cmH_2O, $P < 0.001$) but did not alter heart rate, systemic blood pressure, mean pulmonary arterial pressure, or right ventricular end-diastolic pressure. This response was not abolished by local application of lidocaine to the MPA. In three cats input impedance was calculated from measurements of pressure and flow in the MPA. Impedance was calculated with flow measured using an EMF and ultrasonic volume flow probe (USF), which avoids the constraining effect of the EMF. When flow was measured with an EMF rather than a USF, there was a significant difference in the impedance spectra ($P < 0.001$), but it was only apparent in the moduli greater than six harmonics. We conclude that the EMF does affect right ventricular afterload in acute experiments and alters the measured input impedance.

cats; dogs; ultrasonic flow probe; input impedance; mathematical models

PERIVASCULAR ELECTROMAGNETIC FLOW probes (EMFs) have been used for many years to measure instantaneous blood flow without requiring the vessels to be cannulated (10, 12, 17). The rigid cuff containing the electrodes and magnet is molded with a cylindrical center so that it can be placed around the vessel. As a result, lateral wall excursion of the vessel due to pulsatile flow is limited because the probe effectively stiffens the vessel over the area to which it is applied. In acute preparations, it is necessary to use a flow probe that slightly constricts the vessel at the site to which it is applied because the silver electrodes must maintain close contact with the vessel wall. Although this constriction has little effect on resistance, it decreases compliance by reducing the cross-sectional area and increases local inertance. These problems are well recognized (3, 13, 14, 16) and are thought to be minor (12) but difficult to investigate because there had been no readily available alternative to the cuffed EMF for measuring instantaneous blood flow directly.

Recently, an ultrasonic transducer for measuring flow rather than velocity has become available commercially; the ultrasonic flow probe (USF) can be used without distorting the vessel wall or constraining lateral wall motion (5). The USF has been validated against blood flow measurements made with an EMF in systemic arteries (7, 9), an indicator dilution method (6), and a microsphere technique (2). We predicted from a mathematical model that the constraining effect of the EMF would alter input impedance. The predominant effect would be an increase in the moduli at high frequencies. As a result of these changes, we predicted that there would be an increase of pulmonary arterial pulse pressure and mean right ventricular pressure.

To test these predictions, two groups of experiments were performed. The first group of experiments was conducted in dogs in which we compared pulmonary hemodynamic measurements made with and without an EMF around the main pulmonary artery. The second group of experiments was conducted in cats in which we compared pulmonary arterial input impedance when flow was measured by an EMF with impedance measured by a USF. In the APPENDIX we describe the mathematical model and the predicted changes of the impedance spectrum that are expected when flow is measured with an EMF rather than a USF. In addition, we estimated the extent to which these changes are due to constricting the diameter of the vessel and to stiffening of the vessel wall.

METHODS

Experimental preparation in dogs. Anesthesia was induced in dogs weighing 15–20 kg with thiamylal sodium (6 mg/kg iv, Bio-Ceutic) and α-chloralose-borate solution (2 ml/kg). The solution contained α-chloralose (60 mg/ml, Sigma Chemical), sodium tetraborate decahydrate (46 mg/ml, Sigma Chemical), and sodium bicarbonate (25 mg/ml). Anesthesia was then maintained with a continuous infusion of a 1:1.85 dilution of that solution at a rate of 1.32 ml/kg body wt/h. The animals were ventilated with a Harvard pump through an endotracheal tube at a rate of 12–14 breaths/min with a tidal volume

of ~20 ml/kg. A femoral vein catheter was inserted for administration of pancuronium bromide (0.1 mg/kg) to induce muscular paralysis, which was repeated as required. A left thoracotomy was performed at the fifth intercostal space. The pericardium was incised, and the trunk of the main pulmonary artery and the left lower lobe pulmonary artery were dissected free from surrounding tissues. EMFs (Statham SP7515 series) were placed around both these vessels, with the largest probe used to produce a flow signal throughout the respiratory cycle. Probes that are too large may transduce a flow signal during inspiration but not during expiration when electrical contact is lost because of a decrease in pulmonary arterial pressure and diameter. An EMF was placed around the pulmonary artery to the left lower lobe to estimate the proportion of pulmonary blood flow to the left lower lobe ($\dot{Q}_{LLL}$) during diastole and to measure mean $\dot{Q}_{LLL}$, which was used as an indicator of changes of cardiac output. For measurement of blood flow in the main pulmonary artery, we used one of the following sizes of EMF: *1*) 14-mm luminal diam, 12-mm length, 22.3-g wt, *2*) 16-mm luminal diam, 12-mm length, 23.3-g wt, or *3*) 18-mm luminal diam, 12.5-mm length, 24.7-g wt. For measurement of the pulmonary blood flow to the left lower lobe, we used an EMF of either 5-mm luminal diam, 4-mm length, 17.3-g wt or 6-mm luminal diam, 5-mm length, 18.8-g wt. A catheter pressure transducer (Millar model PC-330) was inserted through a purse-string suture in the pulmonary conus, and the transducer tip was positioned as close as possible to the midpoint of the EMF on the main pulmonary artery. All electrical signals were passed directly to an analog-to-digital conversion board (Data Translation DT2801A) in a Wells American A Star computer and displayed on an eight-channel Gould recorder. The hemodynamic variables that we calculated were mean pulmonary arterial pressure, mean pulmonary blood flow, mean pulmonary arterial pulse pressure, heart rate, mean systemic blood pressure, mean right ventricular pressure, right ventricular end-diastolic pressure, and mean $\dot{Q}_{LLL}$. In addition, the proportion of $\dot{Q}_{LLL}$ during diastole was estimated from the contour of the flow waveform of $\dot{Q}_{LLL}$. The integral of flow between the dicrotic notch and end diastole was expressed as percent of the integral of flow throughout the cardiac cycle. Because of the different effects of wave propagation at different frequencies, this calculation can only be considered as an approximation of the true proportion of $\dot{Q}_{LLL}$ during diastole. Each of these measurements was obtained by averaging over 10 cardiac cycles. Each cycle was selected at end expiration of 10 successive breaths.

Protocol. The protocol in these experiments was to make pulmonary hemodynamic measurements with, without, and again with the EMF around the main pulmonary artery. The EMF around the pulmonary artery to the left lower lobe remained in position throughout the experiment.

Because the presence of an EMF may excite a change in smooth muscle tone locally and thereby alter the right ventricular afterload, we conducted additional experiments in a second group of three dogs. We compared the changes in pulmonary hemodynamics that occur with placement of the EMF before and after load application of 4% lidocaine solution to the main pulmonary artery. We made repeated hemodynamic measurements with and without the EMF probe in place. A gauze square soaked with 4% lidocaine was then applied for 15 min around the wall of the main pulmonary artery where the EMF has been positioned. We then repeated the sequence of measurements with and without the EMF. The effect of the EMF on hemodynamic variables was assessed by analysis of variance with a four-factor experimental design. The four factors were *1*) the presence (or absence) of the probe, *2*) the application of local anesthetic, *3*) experimental preparation (between dog variance), and *4*) an interaction effect to determine whether local anesthesia had any influence on the hemodynamic effects of the probe. In a third group of three dogs, we measured the diameter of the main pulmonary artery with a pair of ultrasonic crystals sutured to the adventitia (15). The crystals were then removed, and an EMF was placed at the same site to determine the reduction in mean diameter that is required to obtain a satisfactory flow signal in the main pulmonary artery.

Experimental preparation in cats. Anesthesia was induced with ketamine (20 mg/kg im, Parke-Davis) and maintained with α-chloralose (0.67 ml/kg iv). A midline thoracotomy was performed, pericardium was opened, and the main pulmonary artery was dissected free of surrounding tissue. Pancuronium bromide (0.1 mg/kg iv) was used for muscular paralysis. The animals were ventilated through a tracheal cannula at ~12 breaths/min with a tidal volume sufficient to maintain an arterial P_{CO_2} of 40 Torr. The animals were ventilated with 100% O_2 through a Harvard ventilator (model 618) to which was attached a microswitch producing a 5-V pulse to signal end expiration. Additional simultaneous injections of chloralose and pancuronium bromide were given as needed throughout the experiment through a femoral venous catheter. Pulmonary arterial blood flow was measured with a flow probe around the main pulmonary artery. Two types of flow probes were used, a USF and an EMF. The USF that we used (Transonics, Ithaca, NY) is comprised of an ultrasound transmitter receiver unit (21 × 15 × 7 mm). It was not possible to use the USF with the EMF in situ because of the large size of this unit relative to the length of the feline main pulmonary artery. The unit was positioned over, but not in contact with, the main pulmonary artery by means of a 13-mm square bracket around the artery. The USF was activated with a Transonics Systems (T201) flowmeter. The USF was coupled to the vessel with acoustic jelly. We used the largest EMF that provided a flow signal throughout the respiratory cycle. One of the following sizes was used: *1*) 6-mm luminal diam, 5-mm length, 18.8-g wt, *2*) 7-mm luminal diam, 5-mm length, 19-g wt, or *3*) 8-mm luminal diam, 5.5-mm length, 19.7-g wt. Pulmonary arterial pressure was measured with a catheter pressure transducer (Millar model PC-330). The electrocardiogram was monitored throughout the experiment. All electrical signals were digitized at a sampling rate of 500 Hz. Single heart cycles were selected from 10

successive breaths at end expiration so that impedance could be estimated from the fourier series of the flow signal corrected for the phase lag due to the Statham flowmeter (SP2202). Details of the method of calculating input impedance have been described elsewhere (8).

Protocol. In each animal input impedance was measured with flow measured by the USF and with the flow measured by the EMF. We used the same USF in each experiment, but we used the largest EMF that was capable of providing a flow signal throughout the respiratory cycle. In each of the three cats we alternated the measurement of flow between the EMF and USF on three successive occasions. Therefore we obtained a total of nine measurements of impedance with the EMF and nine measurements with the USF.

Data analysis. We measured mean pulmonary arterial pressure, flow, pulmonary arterial pulse pressure, and impedance with both types of flow probes. Statistical comparison was made by a two-way analysis of variance. To determine whether the measured impedance was dependent on the type of flow probe, we used analysis of variance. To determine whether the anticipated change in the measured input impedance occurred (see APPENDIX), we compared the relation between the moduli and frequency for impedance with flow measured with the USF and for impedance with flow measured by the EMF using analysis of covariance. In all cases, statistical significance was accepted at the 5% level.

RESULTS

Effect of EMF. The effects of the EMF on pulmonary hemodynamics in dogs are shown in Fig. 1. When the EMF is placed around the main pulmonary artery, there is an increase in pulse pressure but no change in mean pulmonary arterial pressure or mean $\dot{Q}_{LLL}$, which is used as an index of cardiac output. The increased pulse pressure was associated with a reduction in the proportion of $\dot{Q}_{LLL}$ that occurs during diastole. The increase in pulse pressure was largely due to an increase in systolic pressure from 38.5 to 42.0 cmH_2O ($P < 0.02$); the decrease in diastolic (from 20.7 to 20.1 cmH_2O) was not significant. Placement of the EMF had no significant effect on heart rate (from 146 to 145 min^{-1}), mean femoral arterial blood pressure (from 131 to 129 mmHg), or right ventricular end-diastolic pressure (from 7.9 to 7.4 cmH_2O).

To determine the reduction in pulmonary arterial diameter when an EMF is used, measurements were made in the second group of dogs (Table 1). On average, the external diameter of the main pulmonary artery decreased by 10% with placement of the EMF. The increase in pulse pressure averaged 18%, which is a similar order of magnitude that was observed in the preceding experiments.

A third group of dogs was used to determine whether topical lidocaine at the site of EMF placement would abolish this marked increase in pulse pressure. Although there were statistically significant increases in pulse pressure with placement of the flow probe, lidocaine had no significant effect on this response (Fig. 2).

Comparison of impedance spectra obtained by EMF and USF. Figure 3 shows examples of the pressure and flow

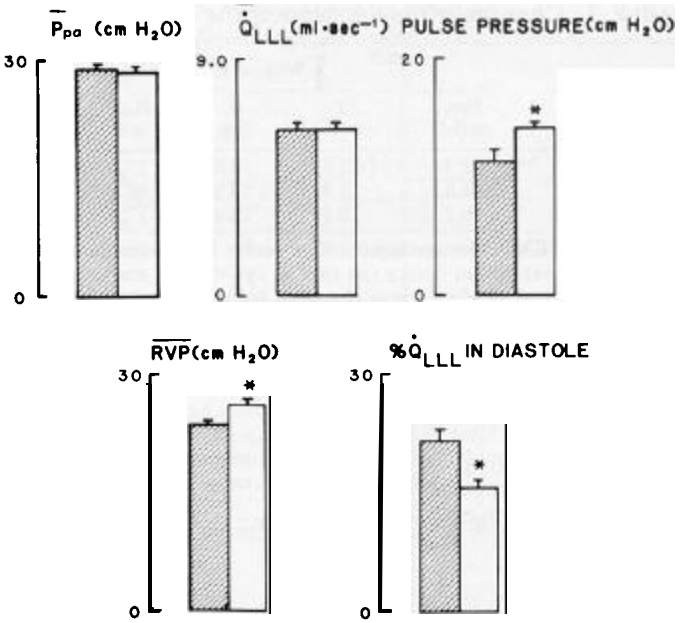

FIG. 1. Effect of electromagnetic flow probe on pulmonary hemodynamics. Five bar charts show changes (means ± SD) of mean pulmonary arterial pressure ($\bar{P}pa$, cmH_2O), mean pulmonary blood flow to the left lower lobe ($\dot{Q}_{LLL}$, ml/s), pulmonary arterial pulse pressure (cmH_2O), mean right ventricular pressure ($\overline{RVP}$, cmH_2O), and the percentage of $\dot{Q}_{LLL}$ that occurs during diastole. ▨, Measurements obtained when electromagnetic flow probe was removed from main pulmonary artery ($n = 7$). □, Measurements obtained with electromagnetic flow probe in place ($n = 14$). * Significant increases in pulse pressure and right ventricular pressure and significant decrease in percent $\dot{Q}_{LLL}$ during diastole ($P < 0.05$).

waveforms obtained in an experiment in a cat. Table 2 shows measurements of pulmonary hemodynamics when flow is measured with the USF and with the EMF. There was no significant difference in mean pulmonary arterial pressure or flow when the flow probe was changed from USF to EMF, but there was a significant increase in pulse pressure due to the distorting effects of the EMF. Figure 4 shows that the predominant difference between the impedance spectra when flow is measured with EMF rather than USF is an increase of the moduli at high frequencies. At high frequencies the signal power decreases, which results in a low signal-to-noise ratio. The statistical approach that we used rejects higher harmonics when a mean phase angle can no longer be identified (8). The highest acceptable harmonic in these spectra ranged between 8 and 20 harmonics. We selected the median value (12 harmonics) for this analysis to avoid discarding acceptable data. Even if we choose eight harmonics as our upper limit, analysis of variance still yields a significant difference in the moduli between the EMF and USF measurements ($P < 0.05$). The slope of the relation between moduli and frequency was significantly greater for the impedance spectra with flow measured by EMF than for spectra with flow measured by USF ($P < 0.001$). This difference was significant by analysis of variance ($P < 0.001$). Analysis of covariance showed that the relation between moduli and frequency is fitted best with a linear relation for USF but with a quadratic relation for the EMF because of the increased moduli at high frequencies >20 Hz.

TABLE 1. *Changes of the diameter of the main pulmonary artery due to placement of an EMF*

Body Wt, kg	Without EMF					With EMF			Change		
	Ppa, cmH_2O	PP, cmH_2O	D, mm	D_{max}, mm	D_{min}, mm	Ppa, cmH_2O		D, mm	Ppa, Δ%		D, Δ%
19.0	22.2	11.9	16.8	17.6	16.1	22.1	13.2	16	0	11	−5
19.0	30.3	18.3	18.5	20.5	16.2	30.3	19.8	16	0	8	−14
16.6	19.7	10.4	15.9	17.2	15.1	18.6	14.1	14	−6	36	−11

$n = 3$ dogs. EMF, electromagnetic flow probe; Ppa, pulmonary arterial pressure; PP, pulse pressure; D, mean diameter of the main pulmonary artery at end expiration during the cardiac cycle; D_{max}, maximum diameter of the main pulmonary artery at end expiration during the cardiac cycle; D_{min}, minimum diameter of the main pulmonary artery at end expiration during the cardiac cycle.

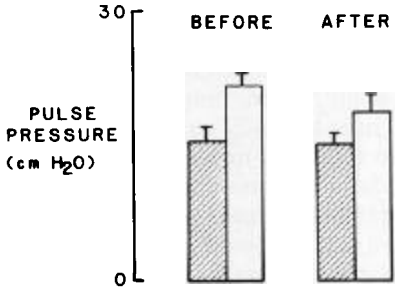

FIG. 2. Effect of local anesthetic on change in pulmonary pulse pressure due to placement of an electromagnetic flow probe. ▨ and □, Measurements made without and with placement of flow probe around main pulmonary artery, respectively.

TABLE 2. *Comparison of pulmonary hemodynamics with EMF and USF in cats*

Condition	Heart Rate, min^{-1}	Ppa, cmH_2O	$\dot{Q}$, ml/s	Rp, units	PP, cmH_2O
EMF	203±11	32.5±2.1	4.7±1.2	7.26±2.65	19.7±6.7
USF	207±11	31.6±1.9	3.7±1.2	7.14±3.94	15.8±5.1*

Values are means ± SD; $n = 9$. $\dot{Q}$, pulmonary blood flow; Rp, input resistance; USF, ultrasonic volume flow probe. For definitions of other abbreviations, see Table 1 footnote. * Significantly different hemodynamic variable measured with EMF in place compared with USF ($P < 0.001$).

DISCUSSION

Effect of EMF placement on pulmonary hemodynamics. We used the largest EMF capable of providing a consistent flow signal throughout the respiratory cycle. The Statham flow probes (SP7515 series) are available in 2-mm increments between 10- and 18-mm luminal diam and in 1-mm increments between 4- and 8-mm luminal diam. It is possible that some restriction of the main pulmonary artery occurs because the increments are too large. The worst possible case in this study would be the application of an EMF of 6-mm luminal diam to a 6.99-mm-OD main pulmonary artery. This circumstance would result in a 14% reduction in vascular diameter, which is still less than the 15% limit proposed by Spencer and Denison (16). In fact, we found that a reduction in main pulmonary arterial diameter of ~10% is required for the measurement of flow with an EMF. Therefore we do not believe that our use of EMF resulted in an excessive reduction of vascular diameter.

Placement of the EMF did not alter mean pulmonary arterial pressure or mean $\dot{Q}_{LLL}$. The EMF caused a 25% increase in pulmonary arterial pulse pressure and a decrease in the proportion of $\dot{Q}_{LLL}$ occurring during diastole. These results are consistent with the idea that the

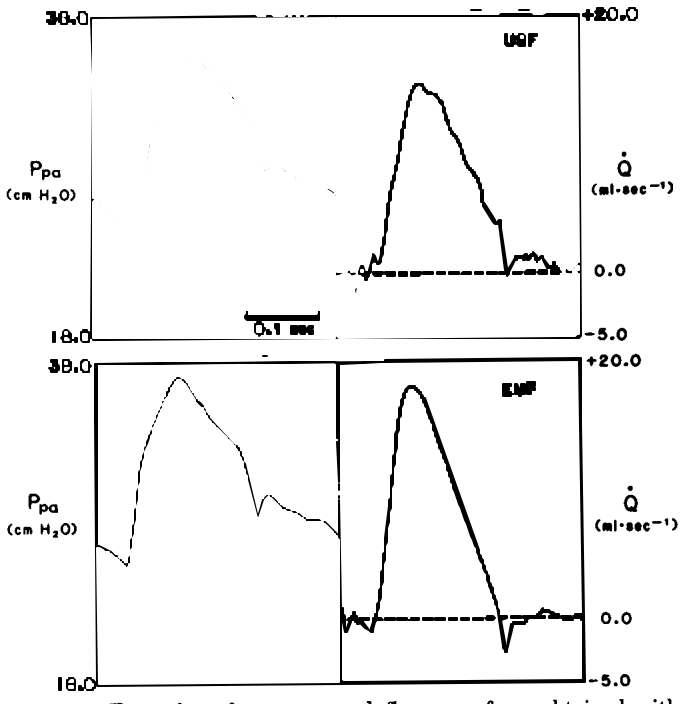

FIG. 3. Examples of pressure and flow waveform obtained with ultrasonic flow probe (USF, *top*) and electromagnetic flow probe (EMF, *bottom*) in main pulmonary artery. Each waveform is raw data ensemble averaged over 10 heart cycles selected from end expiration without any additional filtering. Note increased pulse pressure with EMF. Ppa, pulmonary arterial pressure; $\dot{Q}$, blood flow.

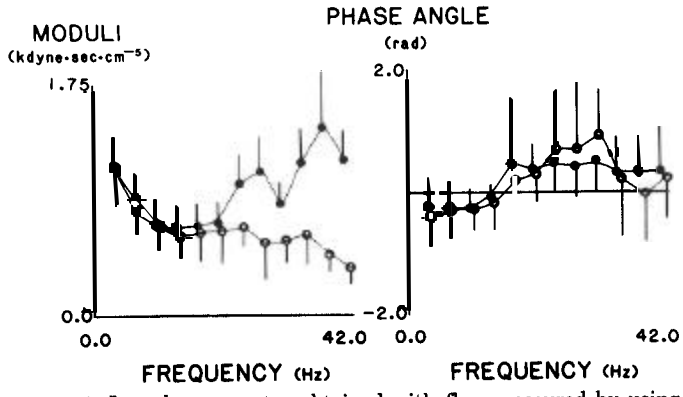

FIG. 4. Impedance spectra obtained with flow measured by using ultrasonic flow probe (USF, ○) and electromagnetic flow probe (EMF, ●). Each spectrum is mean of 9 measurements. *Left*: each modulus is plotted as mean; bar, SE. *Right*: phase is plotted as mean angle; bar, 95% confidence limits of mean by use of angular statistics as described previously (4).

EMF has reduced the compliant properties of the main pulmonary artery, thereby reducing the effectiveness of the Windkessel. The amount of blood that is stored in the stiffened pulmonary trunk during systole is reduced. As a result, there is less of a dampening effect on pulse pressure by the Windkessel and the amount of blood flow that occurs during diastole in the left lower lobe pulmonary artery is reduced.

The results suggest that the EMF caused an increase in pulmonary arterial input impedance. The increase in mean right ventricular pressure would support this notion. Nevertheless these hemodynamic changes could be attributed to changes other than an alteration of right ventricular afterload.

Changes in pulse pressure could result from a change in heart rate, but no significant change occurred when the EMF was removed. An increase in mean right ventricular pressure could result from an increase in preload. However, there is no reason to suppose that the placement of the EMF altered right ventricular preload; indeed we found no significant change in right ventricular end-diastolic pressure. It is possible that the placement of the EMF stimulated receptors on the pulmonary trunk, which, in turn, altered myocardial function by a reflex effect. Although the pulmonary trunk is well innervated with baroreceptors (4), we believe this explanation is unlikely because the same hemodynamic changes were recorded after local anesthetic was applied to the pulmonary trunk, which has been shown to suppress reflexes that occur after mechanical stimulation of receptors in the main pulmonary artery (1, 11). The data indicate that placement of the EMF on the main pulmonary artery alters right ventricular afterload due to a mechanical effect.

Effect of EMF flow on input impedance. If the EMF alters right ventricular afterload, then it might be expected that the EMF would affect the measurement of pulmonary arterial input impedance. To test this idea we compared pulmonary arterial input impedance when flow was measured by an EMF with impedance when flow was measured by a USF, which does not have a local distorting effect on the pulmonary vasculature. As predicted, we found that the moduli for impedance spectra with flow measured by EMF became greater than the moduli with flow measured by USF as frequency increases.

Practical implications. For acute experiments, the USF would appear to be superior to the EMF because it avoids distorting the pulmonary vasculature. Nevertheless, there are some practical limitations. The USF is not suitable for use in acute experiments with prolonged protocols because the acoustic jelly tends to liquify with a resulting loss in the flow signal. We did not compare the two types of probes in chronic experiments where it is not necessary to constrict the vessel when positioning the EMF, because air between the EMF and vessel wall is absorbed during the postoperative period. Our theoretical results suggest that the major distortion from the EMF is due to reduction in local vascular diameter rather than the splinting effect that it has on the vascular wall. Therefore, in chronic experiments, we would anticipate that the distorting effects of the EMF would be reduced considerably.

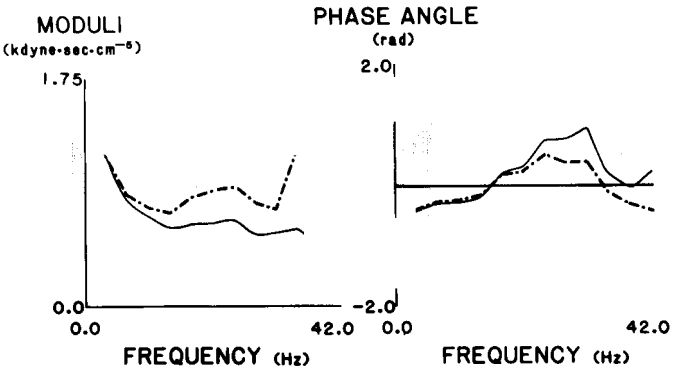

FIG. A1. Comparison of effect of electromagnetic flow probe on impedance. ——, Spectrum shown in Fig. 4 with flow measured by use of ultrasonic flow probe without distortion of main pulmonary artery; -·-·-, same spectrum modified to simulate circumstance if flow was measured with an electromagnetic flow probe.

APPENDIX

Predicted Effects of EMF on Impedance

We used the input impedance measured with the USF (Fig. 4) for these calculations. We assumed that there was no distortion of the main pulmonary artery associated with using this probe. To calculate impedance as if flow had been measured with an EMF, we first calculated the impedance at the distal end of the main pulmonary artery at its bifurcation. We then altered the physical properties of the main pulmonary artery at the site of the EMF and recalculated the input impedance. It was assumed that impedance is measured at the midpoint of the main pulmonary artery, which was 1 cm long with a 0.7 cm ID at zero transmural pressure (D_o) and that it has a linear diameter-pressure relation with slope of 0.6081 $\Delta D_o\%/\text{cm}H_2O$ based on our own measurements in vivo (unpublished observations). From these data, we estimated the characteristic impedance (Z_c) and the propagation coefficient (γ) as described previously (8). Both Z_c and γ are complex numbers and are functions of ω, which is the angular frequency ($2\pi f$), where f is the frequency. We then estimated the reflection coefficient (Γ), which also is a complex number and a function of ω.

$$\Gamma = (Z_i - Z_c)\exp(2\gamma L)/(Z_i + Z_c) \qquad (A1)$$

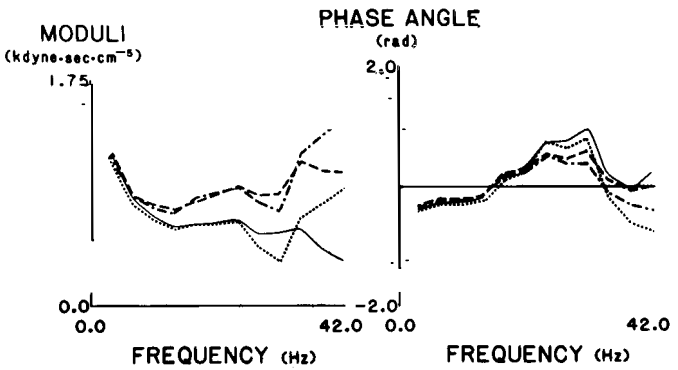

FIG. A2. Analysis of constraining and constricting effects of electromagnetic flow probe (EMF) on impedance. ——, Impedance measured with ultrasonic flow probe; . . . ., impedance modified by constraining effect of EMF; - - -, impedance modified by constricting effect of EMF; -·-·-, impedance with both constricting and constraining effect of EMF.

where Z_i is the input impedance at the point of measurement and L is the distance between this point and the bifurcation of the main pulmonary artery. Γ was used to estimate the impedance at the bifurcation, which is the terminal impedance (Z_t)

$$Z_t = Z_c(1 - \Gamma)/(1 + \Gamma) \qquad (A2)$$

The impedance at the bifurcation was used as a starting point to estimate the impedance if an EMF had been used to measure flow. The pulmonary artery was divided into four sections: from the bifurcation to the distal end of the EMF (L_1), from the distal end to midpoint of the EMF (L_2), from the midpoint to the proximal end of the EMF (L_3), and from the proximal end to the origin of the main pulmonary artery (L_4). L_1 and L_4 are each 2 mm long; L_2 and L_3 are 3 mm each. The input impedance for L_1 and L_2 are calculated from its Z_c, γ, Γ, and L according to the following equation

$$Z_i = Z_c\,[1 + \Gamma\exp(-2\gamma L)]/[1 - \Gamma\exp(-2\gamma L)] \qquad (A3)$$

where $\Gamma = (Z_t - Z_c)/(Z_t + Z_c)$. *Equation A3* is first applied to section L_1 and then to L_2. The Z_i of L_1 becomes the Z_t of L_2. For section L_2, Z_c, Γ, and γ are recalculated to take into account the distorting effects of the EMF, which have been considered as two components: a constricting effect and a constraining effect. The constricting effect of the EMF reduces the diameter of L_2 by 9.4%. This value is well within the 15% reduction in diameter mentioned by Spencer and Denison (16) as being the upper limit that would avoid interference with flow pulsations. The constraining effect of the EMF on section L_2 is simulated by a 99% reduction of change of diameter per unit change of pressure (dD/dP). By applying these revised values of Z_c, Γ, and γ to *Eq. A3*, we calculated the Z_i for L_2, which is the expected impedance if the EMF had been used to measure flow. Figure A1 shows how the distorting effect of the EMF modifies the measured input impedance. Although there is a small decrease in phase angle at high frequencies, the predominant effect appears to be an increase in the moduli as frequency increases.

In addition, we estimated the constricting and constraining effects of the EMF on impedance separately. Figure A2 shows the relative contributions of these two effects; the major effect is due to constriction.

It should be emphasized that this linear approach has a number of simplifying assumptions: more importantly, laminar flow and a cylindrical uniform main pulmonary artery. Furthermore the Womersley equations neglect local convective acceleration. Therefore the results from the calculations can be considered only as approximate.

We thank the Transonics Systems of Ithaca, New York for loaning the ultrasonic flow probe and flowmeter. We thank Steve Neth, Constantina Theophilos, and Amy Wurtenberger for expert technical assistance.

This work was supported by a grant from the Whitaker Foundation, a grant-in-aid from the American Heart Association (83-1187) and, in part, from the West Palm Beach Chapter. Support was also received from National Heart, Lung, and Blood Institute Research Career Development Award HL-01418 (B. J. B. Grant), an American Lung Association Research Fellowship (J. M. Fitzpatrick), and the Parker B. Francis Foundation (L. J. Paradowski).

Received 21 September 1987; accepted in final form 26 April 1988.

REFERENCES

1. ARAMENDIA, P., C. TAQUIRI, A. FOURCADE, AND A. TAQUINI. Reflex vasomotor activity during unilateral occlusion of the pulmonary artery. *Am. Heart J.* 66: 53–60, 1963.
2. BARNES, R. J., R. S. COMLINE, A. DOBSON, AND C. J. DROST. An implantable transit time ultrasonic blood flow meter. *J. Physiol. Lond.* 345: 2–3, 1983.
3. CAMPBELL, K. B., J. A. RUGO, P. A. KLAVARO, J. D. ROBINETTE, AND J. E. ALEXANDER. Aortic bulb-aortic orifice hemodynamics in left ventricle-systemic arterial interaction. *Am. J. Physiol.* 248 (*Heart Circ. Physiol.* 17): H132–H142, 1985.
4. COLERIDGE, J. C. G., AND C. KIDD. Electrophysiological evidence of baroreceptors in the pulmonary artery of the dog. *J. Physiol. Lond.* 150: 319–331, 1960.
5. DROST, C. J. Vessel diameter—independent volume flow measurements using ultrasound. In: *Proceedings of San Diego Biomedical Symposium.* San Diego, CA: San Diego Biomed. Soc., 1978, vol. 17, p. 299–302.
6. EISEMANN, J. H., G. B. HUNTINGTON, AND C. L. FERRELL. Blood flow to hindquarters of steers measured by transit time ultrasound and indicator dilution. *J. Dairy Sci.* 70: 1385–1390, 1987.
7. GOREWIT, R. C., D. G. BRISTOL, M. AROMANDO, AND G. G. THOMAS. Mammary blood flow of cows measured by ultrasonic and electromagnetic flow meter (Abstract). *J. Dairy Sci.* 67: 159, 1984.
8. GRANT, B. J. B., AND L. J. PARADOWSKI. Characterization of pulmonary arterial input impedance with lumped parameter models. *Am. J. Physiol.* 252 (*Heart Circ. Physiol.* 21): H585–H593, 1987.
9. HARTMAN, J., J. KOERNER, L. LANCASTER, AND R. GORCZYNSKI. In vivo calibration of a transit-time ultrasound system for measuring ascending aorta volume flow. *Pharmacologist* 27: 127, 1985.
10. KOLIN, A. An electromagnetic flowmeter. Principle of the method and its application to blood flow measurements. *Proc. Soc. Exp. Biol. Med.* 35: 53–56, 1936.
11. LEWIN, R. J., C. E. CROSS, P. A. RIEBER, AND P. F. SALISBURY. Stretch reflexes from the main pulmonary artery to the systemic circulation. *Circ. Res.* 9: 585–588, 1961.
12. MILNOR, W. R. *Hemodynamics.* Baltimore, MD: Williams & Wilkins, 1980.
13. NOBLE, M. I. M., I. T. GABE, AND A. GUZ. Blood pressure and flow in the ascending aorta of conscious dogs. *Cardiovasc. Res.* 1: 9–20, 1967.
14. O'ROURKE, M. F., AND W. F. MILNOR. Relation between differential pressure and flow in the pulmonary artery of the dog. *Cardiovasc. Res.* 5: 558–565, 1971.
15. PAGANI, M., H. BAIG, A. SHERMAN, W. T. MANDERS, P. QUINN, T. PATRICK, D. FRANKLIN, AND S. F. VATNER. Measurement of multiple simultaneous small dimensions and study of arterial pressure-dimension relations in conscious animals. *Am. J. Physiol.* 235 (*Heart Circ. Physiol.* 4): H610–H617, 1978.
16. SPENCER, M. P., AND A. B. DENISON. The aortic flow pulse as related to differential pressure. *Circ. Res.* 4: 476–484, 1956.
17. WETTERER, E. Eine neue Methode zur Registrierung der Blutstromungsge schwindigkeit am uneroffrneten Gefass. *Z. Biol.* 98: 26–36, 1937.